Authors' affiliations

Natalja Petkune, PhD student, Department of Civil Engineering, Kingston University London, Surrey, KT1 2EE, UK, Email: *N.Petkune@kingston.ac.uk*

Ted Donchev, Associate Professor, Department of Civil Engineering, Kingston University London, Surrey, KT1 2EE, UK, Email: *T.Donchev@kingston.ac.uk*

Homayoun Hadavinia, Associate Professor, School of Mechanical & Automotive Engineering, Kingston University London, SW15 3DW, UK, Email: *H.Hadavinia@kingston.ac.uk*

David Wertheim, Professor, Faculty of Science, Engineering and Computing, Kingston University London, Surrey, KT1 2EE, UK, Email: *D.Wertheim@kingston.ac.uk*

Mukesh Limbachiya, Professor, Department of Civil Engineering, Kingston University London, Surrey, KT1 2EE, UK, Email: *M.Limbachiya@kingston.ac.uk*

Performance of pristine and retrofitted hybrid steel / fibre reinforced polymer composite shear walls

Natalja Petkune[1*], Ted Donchev[1*], Homayoun Hadavinia[2], Mukesh Limbachiya[1], David Wertheim[3]

[1] Department of Civil Engineering, Kingston University London, KT1 2EE, UK

[2] School of Mech & Auto Engineering, Kingston University London, SW15 3DW, UK

[3] Faculty of Science, Engineering and Computing, Kingston University London, KT1 2EE, UK

ABSTRACT

In this study new types of advanced hybrid shear wall systems using steel/fibre reinforced polymer (FRP) composites are being developed for deployment in the construction of buildings. The hybrid steel/FRP shear walls made from laminates of steel with either carbon FRP (CFRP) or glass FRP (GFRP) materials. In total six medium-scaled shear wall specimens were manufactured. In the first phase of the study three pristine specimens: steel shear wall (SSW-P), hybrid steel /CFRP shear wall (HSCSW-P) and hybrid steel/GFRP shear wall (HSGSW-P) were tested. In the second phase of the project, the specimens tested in phase one were retrofitted and retested; these specimens were identified as SSW-R, HSCSW-R and HSGSW-R. The structural repair and strengthening of specimens in the second phase was achieved by replacing the damaged infill plates with new infill plates of the same type, strengthening of the vertical steel frame elements with CFRP laminates and GFRP fabric. All shear wall specimens were tested under quasi-static cyclic loading following the ATC-24 protocol. The behaviour and failure modes of the pristine and retrofitted specimens were compared. The results show that the retrofitted specimens with the

* Corresponding authors: Emails: N.Petkune@kingston.ac.uk (Natalja Petkune), T.Donchev@kingston.ac.uk (Ted Donchev)

procedure developed have higher stiffness, higher ultimate loading capacity and similar energy dissipation capability relative to pristine specimens. For hybrid retrofitted specimens the ultimate load capacity increased more than 11% in comparison with pristine hybrid specimens.

Keywords: Steel and hybrid shear wall; Fibre reinforced polymer composite; Medium scale shear wall specimens; earthquake loading; retrofitting.

1 INTRODUCTION

Steel shear walls (SSW), consisting of steel boundary elements and steel infill plate, have good lateral resisting properties and hence they can be used in regions with high levels of seismic activity. Their benefits such as lightweight, high load bearing capacity and high energy dissipation make them an attractive alternative in the construction of high-rise buildings particularly in areas of seismic activity. However, one of the main problems limiting their practical application is difficulty in repairing them after an earthquake event. Since the 1970s, SSWs have been popular in the USA and Japan for construction of high-rise buildings; they provide significant reduction in wall thickness as well as weight of the building and as a result reduction of foundation and inertia loads [1]. Hybrid shear walls (HSW) consisting of steel boundary elements and steel infill plates laminated with fibre reinforced polymers (FRP) on both sides of the plate are in process of the development. The established definition for steel shear walls is a combination of the steel frame with steel infill plate (e.g. see [1, 2, 3] to name a few). In this research the existing definition of steel shear walls was further developed as hybrid shear walls for elements consisting of steel frames and hybrid steel/FRP infill plates in aspect of infill plate modifications.

When buildings are subjected to seismic loading, severe damage to shear walls can occur. It is important to use effective techniques to recover initial strength and stiffness of the shear walls in order to avoid demolition of the building or requirement for introduction of new additional elements. This paper will address the use of the fibre reinforced polymer composites for enhancing the performance of SSW and also for a permanent retrofitting and strengthening of steel and hybrid (steel/FRP) shear walls after earthquake damage. These strengthening methods could also be applied to undamaged structures when changes in the structural loads on an existing building require design of higher capacity SSWs or HSWs.

2 BACKGROUND

FRP materials have been used in civil engineering over several decades for strengthening of reinforced concrete and steel structures, improving capacity of buildings, bridges, dams and other structures. The most common FRP materials used for strengthening purposes are glass FRP (GFRP) and carbon FRP (CFRP). The high tensile strength of FRP and ease of application provides a clear benefit for their use in strengthening of structures. Advantages of FRP over steel as a strengthening material include higher strength-to-weight and stiffness-to-weight ratios, corrosion resistance, ease and speed of transportation and installation, electromagnetic neutrality and ability to follow irregular shapes of structures via wet lay-up- processes.

2.1 FRP strengthening of steel structures

Strengthening of steel structures with FRP in comparison with strengthening steel members by welding additional steel plates can be particularly beneficial in applications where it is important to avoid new residual stresses caused by the welding process and to avoid local strength reductions in heat affected zones [4].

Review of the current applications of steel structures strengthened with FRP by Teng et al. [5] and Zhao and Zhang [6] highlighted that the behaviour of the steel/FRP structural elements depends on the selection of the adhesive with appropriate mechanical properties not only in short-term performance, but also in long-term durability. It is important for bond-critical applications to use appropriate preparation techniques of the steel surfaces before adhesive application.

The main area of applications of using FRP for strengthening of steel structures can be summarised in the following categories:

- strengthening of steel elements against local buckling [7, 8]
- flexural strengthening of the steel beams [9]
- fatigue strengthening for steel beams, steel plates and connections [10, 11]
- strengthening of steel hollow sections and concrete filled steel tubes [12, 13]

Harries et al. [7] conducted experiments on retrofitting columns made of WT steel sections with ultra-high modulus of elasticity GFRP strips, which were tested under concentric cyclic compressive loading to failure. Application of the FRP material prior to the test resulted in delay of the plastic buckling and formation of the plastic “kink” which positively affects energy dissipation and ultimate cyclic ductility properties. Similar conclusions were made by El-Tawil et al. [8]. They investigated the behaviour of three double channel built-up members wrapped with CFRP in the regions of plastic hinges tested under cyclic loading. It was concluded that structural behaviour of CFRP reinforced specimens was considerably better than unreinforced ones. CFRP wrapping in the regions of plastic hinges increased the size of the plastic hinge region and slowed down the occurrence of the local buckling. It also delayed the onset of lateral torsional buckling and resulted in a higher energy dissipation capacity in the plastic hinge regions.

2.2 FRP and steel applications for improving seismic resistance

An important aspect for the use of the FRP is to improve seismic resistance of the existing lateral load resisting system of buildings, particularly for shear walls. Several experimental and numerical studies have been conducted to investigate the behaviour of undamaged steel shear walls [14, 15, 16].

An innovative lateral resisting system in the form of hybrid shear walls (HSW), consisting of steel frames and steel infill plates laminated with FRP, have been investigated by several researchers in the past five years [3, 17, 18, 19, 20]. Experimental studies on the use of hybrid steel/GFRP shear walls showed that they provide higher stiffness, larger energy dissipation capacity and more uniform tension field during loading than steel shear walls with the same thickness of the steel infill plate [17]. Nateghi et al. [18] tested steel shear walls with infill plates laminated with GFRP, reaching a similar conclusion to Maleki et al. [17] that it significantly increases ultimate strength and initial stiffness. Cumulative energy dissipation of the hybrid steel/GFRP shear walls was larger than steel shear walls. Both studies concluded that the fibre orientation plays a significant role in the behaviour of the specimens, and laminates with fibres in the direction of the tension field exhibit better performance.

Use of CFRP in laminating steel plates was initially investigated by Hatami and Rahai [19]. They concluded that HSW with CFRP/steel infill plates in comparison with steel shear walls have higher energy dissipation and enhanced elastic stiffness and shear capacity [19]. Petkune et al. [20] compared the behaviour of both GFRP/steel and CFRP/steel infill plates in HSW design within steel boundary elements. Further, more detailed investigation of the role of boundary conditions [21] in the usage of CFRP or GFRP as an element in hybrid infill plates was presented.

Initial steps in the application of infrared thermography (IRT) for detecting delamination between GFRP and steel in hybrid infill plates are reported in [17]. Petkune et al. [22, 23] have extended this work for detection of delamination in hybrid steel/FRP infill plates using IRT.

2.3 Structural repair of SSW and HSW

Limited studies are available on the structural repair and strengthening of the damaged SSWs to recover their initial capacity after earthquakes. Petkune et al. [24] conducted experimental studies of damaged SSWs with retrofitting the columns and infill plate with GFRP bi-directional fabric and concluded this method to be a suitable temporary retrofitting solution. Load capacity of the retrofitted specimen is increased in comparison with pristine SSW, but it is limited to applications subjected to small displacements. However, more effective permanent strengthening is needed to ensure sufficient capacity and durability after repair [24].

Both structural repair of the specimens and the development of new hybrid elements indicate that simultaneous application of steel and FRP materials in seismic resistant structures could be beneficial. This study aims to develop an effective structural repair technique for SSW and HSW systems using FRP materials.

3 METHODOLOGY

3.1 Description of specimens

Shear wall specimens are scaled models with a height of 1025 mm and width of 1090 mm (see Figure 1). All specimens are made from steel frames and steel or hybrid infill plates. Steel frame members consist of two columns and a beam, all of them made from UB 127 x 76 x 27 sections (S355 grade). The shear wall scaled models were designed at Kingston University London and manufactured by Cannon Steels Ltd. Primary fish plates were welded continuously to the steel frame.

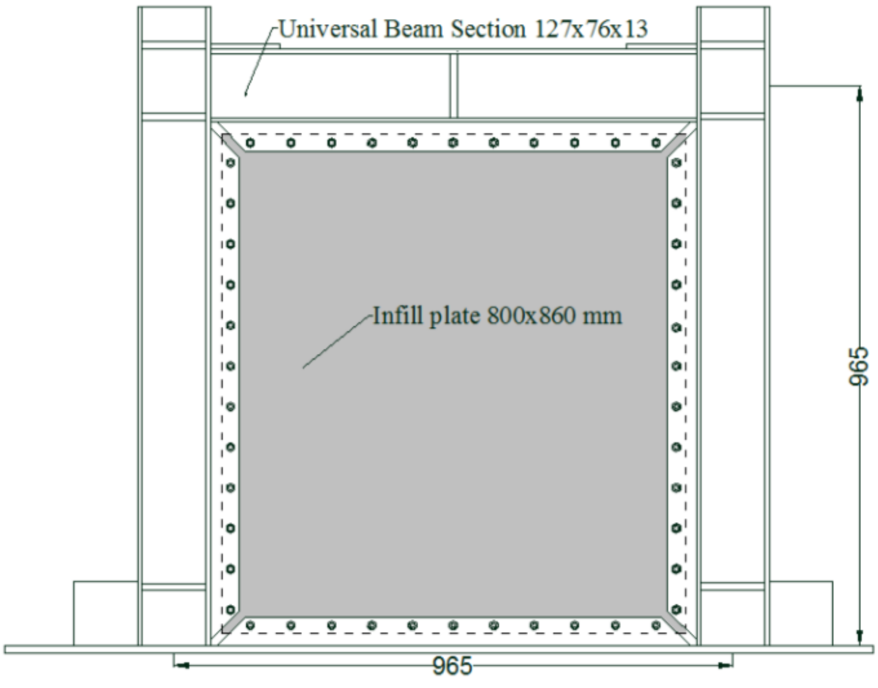

Figure 1. Dimensions of shear wall specimens.

Two different groups of specimens were tested. In the first phase of the programme three pristine specimens: steel shear wall (SSW-P), hybrid steel /CFRP shear wall (HSCSW-P) and hybrid steel/GFRP shear wall (HSGSW-P) were tested. In the second phase of the work, the tested specimens in the first phase were retrofitted and retested. These specimens are identified as SSW-R, HSCSW-R and HSGSW-R. The structural repair of specimens in the second phase was undertaken by replacing the damaged infill plates with new infill plates of the same type, and strengthening the vertical steel frame elements with CFRP laminates and GFRP fabric. The pristine specimens are used as reference specimens to measure the scale of restoration of retrofitted specimens.

The specifications of all specimens are summarised in Table 1.

Table 1. Description of SSW and HSW specimens.

Name of the specimen	Labels	Stacking sequence of the infill plate	Total thicknesses of the infill plate, mm
Steel Shear Wall	SSW-P	Steel [S]	0.80
Retrofitted Steel Shear Wall	SSW-R	Steel [S]	1.40
Hybrid Steel/CFRP Shear Wall	HSCSW-P	[+45/-45/A/S/A/-45/+45]	1.70
Retrofitted Hybrid Steel/CFRP Shear Wall	HSCSW-R	[+45/-45/A/S/A/-45/+45]	1.70
Hybrid Steel/GFRP Shear Wall	HSGSW-P	[+45/-45/A/S/A/-45/+45]	2.40
Retrofitted Hybrid Steel/GFRP Shear Wall	HSGSW-R	[+45/-45/A/S/A/-45/+45]	2.40

Note: A- adhesive film (EF72)

For the steel shear wall (SSW-P) specimen, an infill plate of a 0.8 mm thick from steel grade S275 was used. In the hybrid specimens the same steel frames were used but the infill plates were prepared by symmetrically laminating a steel plate (0.8 mm thick) with two layers of unidirectional (UD) FRP prepreg material on both sides (Figure 2). Unidirectional fibre orientations were placed at $\pm 45^{o}$ relative to the loading direction. The use of the UD FRP prepreg allowed the customization of the infill plates according to design requirement in terms of the fibre orientation and number of FRP layers.

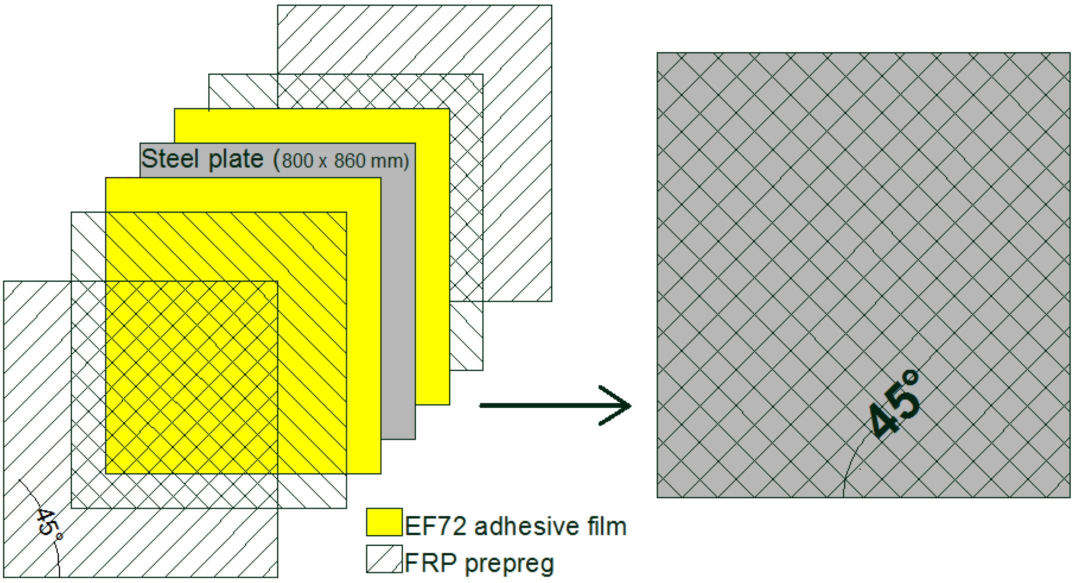

Figure 2. Design specification for hybrid specimens.

For HSCSW-P and HSCSW-R, unidirectional CFRP prepreg type Medium Temperature Molding MTM 28-1 series (produced by Cytec Solvay Group) was laminated on both sides of the steel infill plate. For HSGSW-P and HSGSW-R, unidirectional GFRP prepreg with epoxy resin E722-02 (produced by TenCate Advanced Composites Ltd) was laminated on the both sides of the steel infill plate. The mechanical properties of these prepreg are summarised in Table 2.

Table 2. Mechanical properties of the FRP materials.

	Unidirectional CFRP type MTM 28-1 series prepreg (Cytec Solvay Group)	**Unidirectional GFRP prepreg E722-02 (produced by TenCate Advanced Composites Ltd)**
Young's Modulus E_{11}, GPa	140	41
Young's Modulus E_{22}, GPa	8.5	10.5
Shear Modulus G_{12}, GPa	5.8	3.3
Poisson's ratio ν_{12}	0.319	0.311

For the preparation of hybrid infill plate, FRP layers were laminated according to the manufacturer's recommendations. The infill plates were prepared by thoroughly cleaning the steel plate with sand paper followed by acetone. EF72 adhesive film (manufactured by TenCate Advanced Composites Ltd) with area weight of 100 g/m^2 was placed between the steel plate and FRP prepreg to create a strong bond between FRP laminate and core steel infill plate. The additional adhesive film delays the delamination of FRP prepreg during cyclic loading. Then FRP prepregs were laid according to the design specifications with fibre orientations as indicated in Table 1. The specimen was vacuum bagged and cured inside an oven under vacuum (Figure 3a). The curing temperature increased at a rate of 3^{o}C per minute until 120^{o}C and an even pressure up to 980 mbar was applied to the laminate by using a vacuum pump (Figure 3b). Then the temperature was kept constant at 120^{o}C for 1 hour and finally the temperature decreased to 60^{o}C during the cooling down cycle and the sample was then left to cool to room temperature outside the oven.

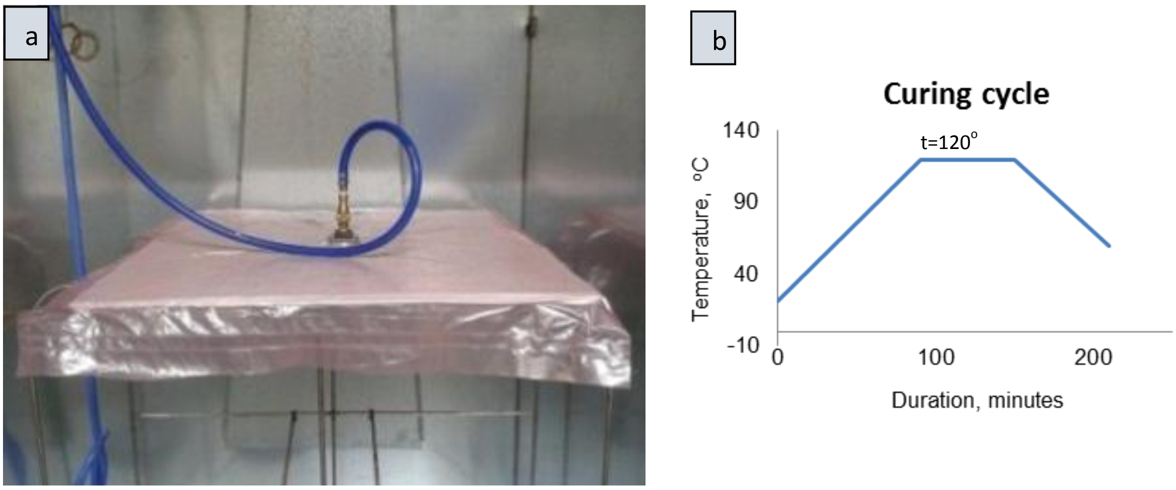

Figure 3. a) oven/vacuum curing of the plate b) curing cycle.

In the steel shear wall specimens, infill plates were bolted to the fish plates (Figure 4a). In the hybrid specimens, in addition to bolts a Devcon epoxy plus adhesive (manufactured by ITW Polymers Adhesives) with a shear strength of 20 MPa was used (Figure 4b) to compensate a relatively weak connection between FRP surface of infill plate and steel surface of fish plates due to the lower coefficient of friction.

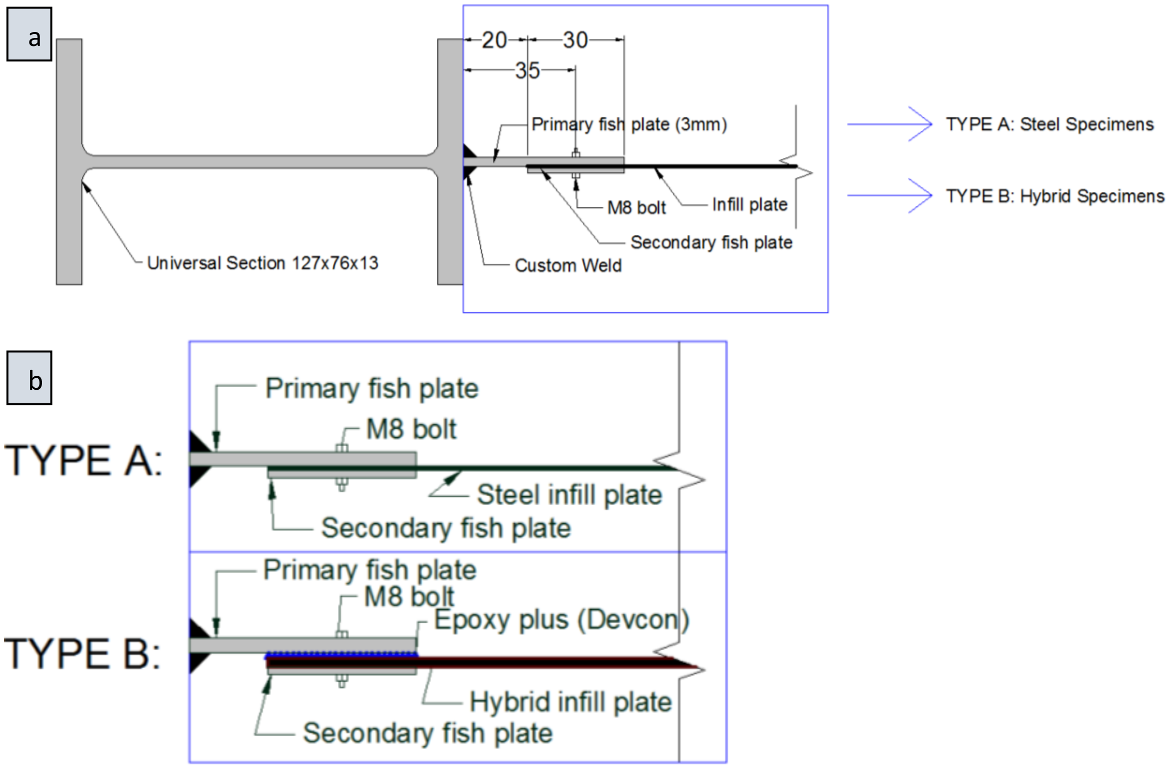

Figure 4. Connection between fish plates and infill plate a) top view of I-beam section and infill plate b) types of connections in steel and hybrid infill plates.

3.2 Retrofitting of tested specimens

The three specimens from the first phase were tested under quasi-static cyclic loading up to a significant level of damage as a result of high in-plane displacement at the top of the frame. For the second phase, these specimens were retrofitted and indicated as SSW-R, HSCSW-R and HSGSW-R.

Table 3. Properties of the FRP materials used for retrofitting of shear walls.

Properties of CFRP laminates [25]		**Properties of GFRP fabric** [26]	
Density, g/cm^3	1.7	Fibre density, kg/cm^3	2.6
Fibre content, v_f %	70	Area weight, g/cm^2	350
Elastic modulus E_f, GPa	165+	Modulus of elasticity E_{cu}, GPa	65+
Tensile strength f, MPa	2800+	Tensile strength f_{cu}, MPa	2000+

The procedure for repairing the original specimens was as following:

- Removal of damaged infill plates
- Strengthening of the frame with CFRP laminates

- Wrapping of the frame with GFRP fabric
- Replacement of infill plate with a new one

Due to the lack of visual damage in the horizontal members of the frame, Weber CFRP S&P CFK 150/2000 unidirectional laminates 1.2 mm thick [25] were attached to the vertical boundary elements only, aiming to cover the area where plastic hinges were formed after previous loading in phase one. The plastic hinges were developed at the bottom and top sections of the vertical elements. The repairs were undertaken by firstly removing the paint with a mechanical wire brush in areas where CFRP laminates and GFRP fabric were planned to be applied. This improved the bonding between the steel and the FRP composites. Then the frame was cleaned with white spirit to remove dust and oil. CFRP laminates were bonded to the frame (Figure 5) with a moisture-tolerant structural adhesive from "Weber". The adhesive has two parts: bisphenol epoxy resin and polyamine hardener, which were mixed with a mass ratio of 2.4:1 according to the supplier's instructions. The adhesive thickness was approximately 3 mm. The A-A section of the I-beam was strengthened with 300 mm (bottom part) and 200 mm (top part) long and 65 mm wide Weber CFRP laminates. The B-B section of I-beam was strengthened with 25 mm wide CFRP laminates with the same lengths as for A-A section. The minimised area of the application of CFRP laminates is adopted from the point of view of more economical strengthening of whole building. In general case if the economy of CFRP laminates is not significant, their application over the whole vertical surface could be beneficial in aspect of improving of their anchorage. Mechanical properties of FRP materials used for retrofitting are tabulated in Table 3.

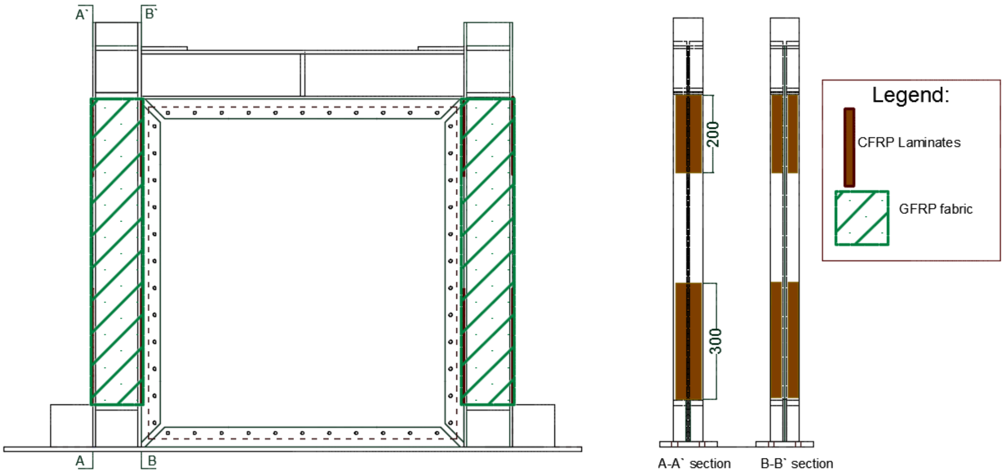

Figure 5. Retrofitting scheme: position of CFRP laminates on shear wall columns (A-A and B-B sections)

After curing of CFRP laminates and adhesive bond, Weber bi-directional woven GFRP wrapping [26] was laid on the frame (Figure 6) using a mixture of epoxy resin and hardener (2:1 by mass ratio). GFRP fabric was applied in two stages: firstly GFRP fabric was applied along the web of the I-beam and along the A-A section of the I-beam as the first layer to allow for proper attachment of the fabric in the areas of internal corners of the section. Then GFRP was wrapped around the whole surface of the columns (Figure 6) as the second layer of GFRP for the areas where first layer is applied. Due to the shape of the I-beam, double wrapping allowed avoidance of “air pockets” in the corners of the section.

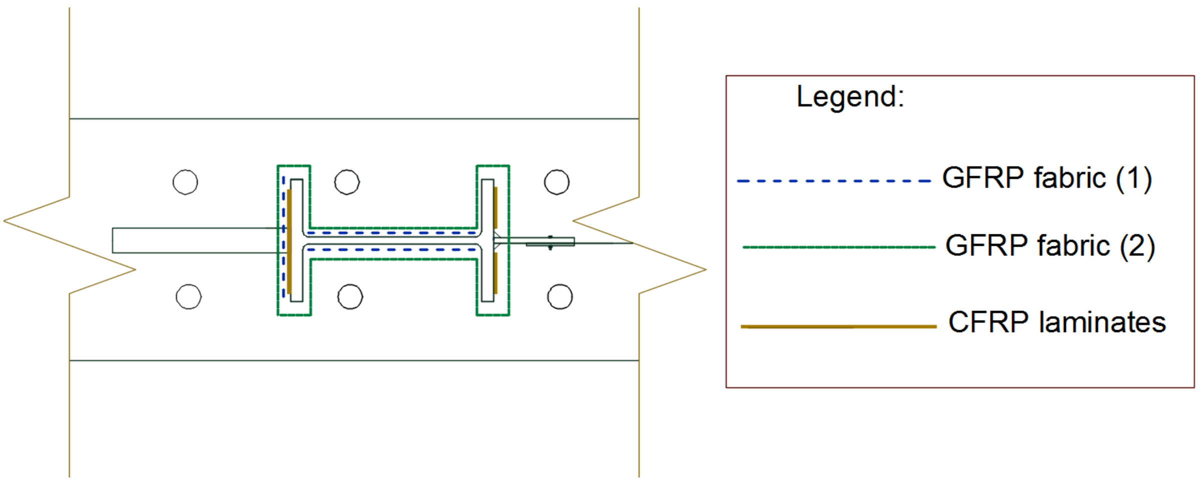

Figure 6. Positioning of CFRP laminates and GFRP fabric on the plan view of the frame

The damaged 0.8 mm thick infill plate from the steel shear wall specimen was replaced with a steel infill plate of thickness of 1.4 mm. The choice of a higher thickness of steel infill plate in this case was due to strengthening considerations. Hybrid specimens were replaced with infill plates with the same steel plate and FRP design specifications as in the pristine specimens.

3.3 Scaled shear wall test set-up and protocol

The scaled shear wall test set-up is shown in Figure 7. The testing rig consists of the reaction frame, loading system and lateral supports. Each of the test specimens was fixed to the bottom part of the reaction frame via high strength bolts and clamps, with lateral supports preventing out-of-plane buckling of the specimen during testing. Shear wall specimens were tested under quasi-static cyclic displacement controlled loading in the in-plane horizontal direction. The loading system consisted of a screw jack, electric motor, gear box and inverter. The applied in-plane force was measured with a 500 kN load cell. Linear variable differential transformers (LVDTs) were used to record displacements. The control LVDT used for measuring displacements in Figures 12, 13 and 14 is indicated as No.10 in Figure 7. Strain gauges were used to record local strain in the plate.

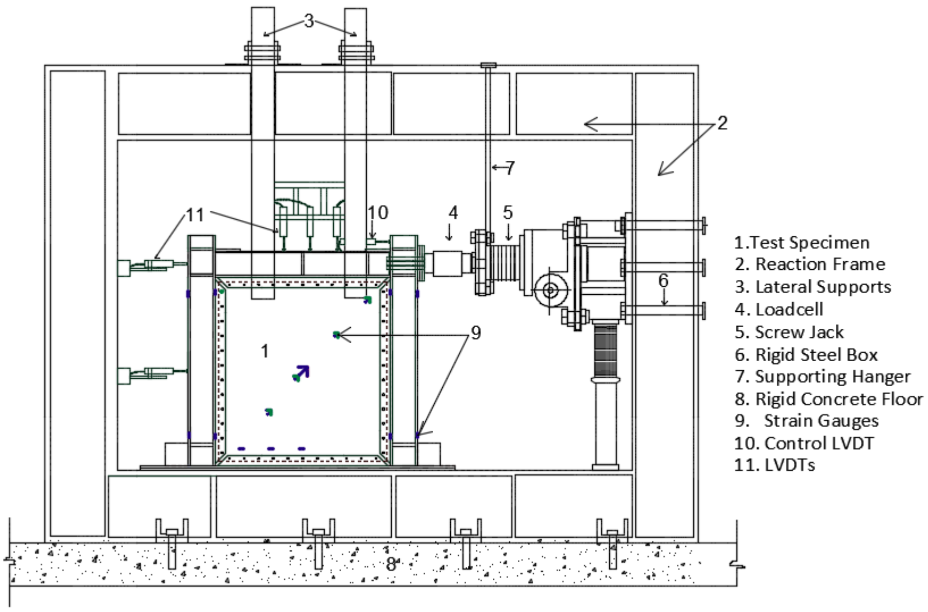

Figure 7. Test set-up for shear wall specimens.

The testing procedure was according to ATC-24 protocol from Applied Technical Council [27]. Figure 8 shows cyclic sinusoidal loading designed for these specific types of specimens and applied for a range of different displacement amplitudes varying from 0.4 mm to 35 mm displacement. The rate of the applying displacement varied from 0.05 mm/min between 0.4 mm and 10 mm displacements to around 2.2 mm/min between 10 mm and 35 mm displacements. Initially, three cycles at each amplitude were applied, and then above 15 mm displacement the number of cycles was decreased to two cycles per amplitude according to the ATC-24 protocol.

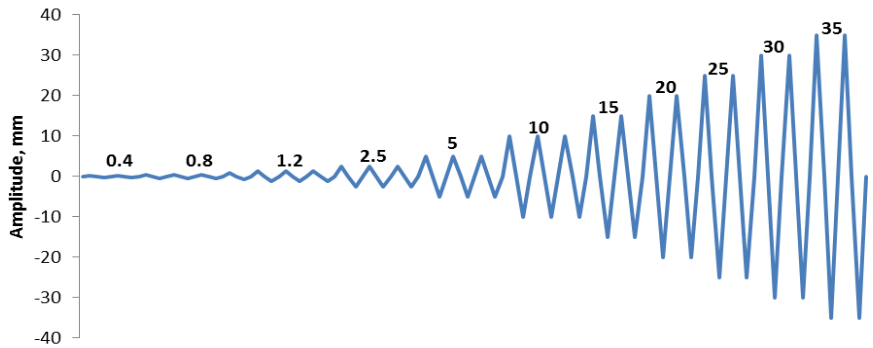

Figure 8. Quasi-static cyclic displacement control loading according to ATC-24 protocol.

4 RESULTS AND ANALYSIS

4.1 Behaviour of pristine and retrofitted specimens

In this section the behaviours of the pristine and retrofitted specimens are discussed including the information about failure mechanisms occurring during the tests. Any changes to infill plates including visual appearance and progression of delamination between FRP layers and steel infill plate, plastic hinges in columns and delamination of the CFRP laminates and GFRP fabric from columns are closely monitored and reported. Furthermore, damage between the infill plate and boundary elements is investigated.

4.1.1 Behaviour of pristine SSW-1 and retrofitted SSW-2 specimens

The pristine steel shear wall specimen SSW-P (Figure 9a) was loaded up to 35 mm displacement. The first signs of buckling of the infill plate occurred at 1.2 mm displacement, which did not fully recover after the end of the 2.5 mm loading cycle. The number and amplitude of diagonal tension field waves were increased at higher displacements. At displacements higher than 10 mm, enlargement of holes around bolts in the connections between fish plates and infill plates started, which led to the yielding of the steel infill plate and its tearing around these areas. In addition sliding of the infill plate progressed with the increase of the displacements. Development of the plastic hinges at the bottom of the columns of the steel frame was noticed at displacements above 15 mm and at the top of the columns with 30 mm displacement. The initial pinching of the infill plate started at a displacement of 15 mm, which further progressed to development of small holes at displacements higher than 30 mm. The final failure of the steel shear wall specimen occurred through the development of the plastic hinges around the bottom and top areas of the column and tearing of the steel plate around bolt holes.

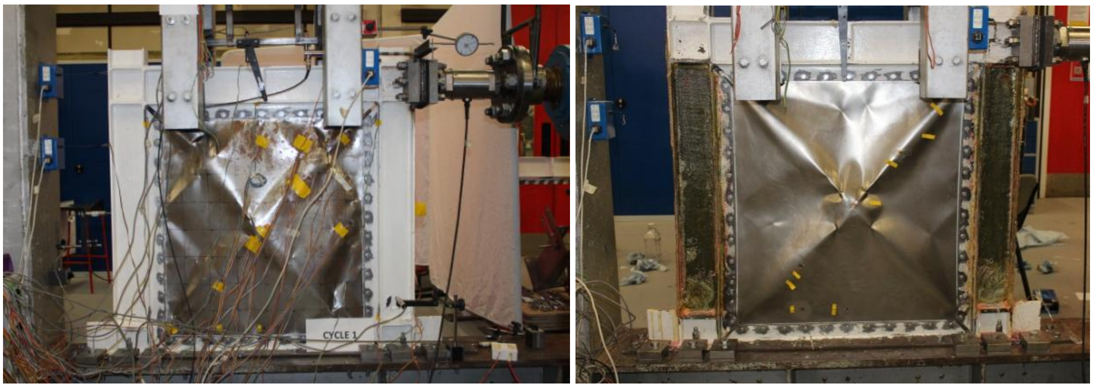

(a) **(b)**

Figure 9. a) Pristine SSW-P and b) retrofitted SSW-R specimens after loaded to 35 mm displacement.

In the retrofitted SSW-P specimen (Figure 9b) visible diagonal tension field development started at a displacement of 3.5 mm in both directions of loading and produced wave-type deformations, which did not fully recover after the end of 3.5 mm loading cycle. Further development of the diagonal tension field was recorded with an increase of the applied displacement. At a displacement of 10 mm, buckling of the primary fish plate occurred where the diagonal tension field waves developed. At displacements above 15 mm, plastic hinges at the bottom of the columns were developed, which led to the development of delamination in GFRP fabric. Sliding between primary fish plates and infill plates was initially recorded for the top and side boundary elements. At 25 mm displacement, development of debonding of the CFRP laminates attached to the top of the columns occurred. With the increase of the loading displacement to 30 mm, further development of the diagonal tension field led to pinching in the centre of the plate with the appearance of small holes. At 35 mm displacement of loading, further progression of the debonding for all CFRP laminates and delamination for GFRP fabric occurred in the lower section of the columns.

4.1.2 Behaviour of pristine HSCSW-P and retrofitted HSCSW-R specimens

In pristine HSCSW-P specimen (Figure 10a) the first sign of buckling of the infill plate through the development of wave-type deformation was noticed at 1.2 mm displacement, which did not recover fully at the end of the applied 2.5 mm displacement cycle. Delamination between FRP and steel plate started in the top corners of the plate along diagonal tension field action, which developed at 10 mm displacement and grew further at higher applied displacement. Sliding and tearing in the connections between fish plates and infill plate started at displacements higher than 15 mm, cracks in the adhesive layer and sliding increased at higher displacement. At 25 mm loading, infill plate had snapped in the top corners near primary fish plates where diagonal tension field was developed with occurrence of holes and delamination of the FRP; elongated bolt holes were visible at displacement of 30 mm. Considerable delamination between CFRP layers and steel plate along the full length of diagonal tension field action and in the corners has been noticed for HSCSW-P at displacement above 25 mm. The specimen was tested up to 30 mm displacement loading.

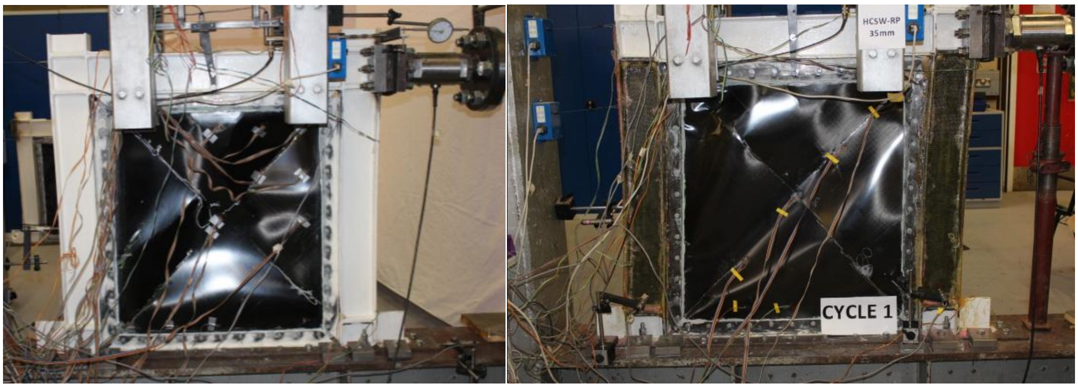

(a) **(b)**

Figure 10. a) Pristine HSCSW-P specimen after loaded to 30 mm displacement b) retrofitted HSCSW-R specimens after loaded to 35 mm displacement.

In retrofitted HSCSW-R specimen (Figure 10b), visible diagonal tension field development started at the displacement of 2.5 mm, the resulting lateral deformations did not fully recover after the end of 2.5 mm loading cycle. Further diagonal tension field waves both in size and number developed with increase of the loading displacement. Other visible changes to the frame and infill plate were noticed at 10 mm displacement, such as cracking in CFRP layers along diagonal tension field action recorded in both directions, which was increased at higher levels of the loading displacement. The integrity of the bond in the connection between fish plates and infill plate was compromised at 15 mm displacement and further cracking in the adhesive developed with increase of the displacements. At 20 mm displacement, cracks in the CFRP layers developed at the bottom part of the infill plate. At 25 mm displacement plastic hinges developed at the bottom of the columns. Similar snapping of the infill plate occurred in the top corners near fish plates, as it occurred in pristine HSCSW-P specimen. Further damage to the connection between infill plates and fish plates occurred at 30 mm displacement, when bolt holes elongations became visible. The test was terminated at 35 mm displacement.

4.1.3 Behaviour of pristine HSGSW-P and retrofitted HSGSW-R specimens

In pristine HSGSW-P specimen (Figure 11a), visible diagonal tension field development started at the displacement of 1.2 mm in both directions, deformations did not fully recover after the end of 2.5 mm loading cycle. At displacement higher than 10 mm, development of tension field residual deformations in both directions led to the delamination of GFRP fabric from steel plate in the top corners of the infill plate. With further loading of the specimen, delamination along diagonal tension field action increased. At 15 mm displacement, cracking in the adhesive layer between fish plates and the infill plate was noticed. First signs of the development of the plastic hinges at the bottom of columns were recorded at 20 mm displacement. At higher displacement delamination was propagated further, however the extent of delamination was smaller compared to pristine HSCSW-P specimen at the same level of loading. At 30 mm displacement, the top corners in the infill plate around fish plates snapped and the elongations of bolt holes of the infill plate became visible. The specimen was tested to 30 mm displacement loading.

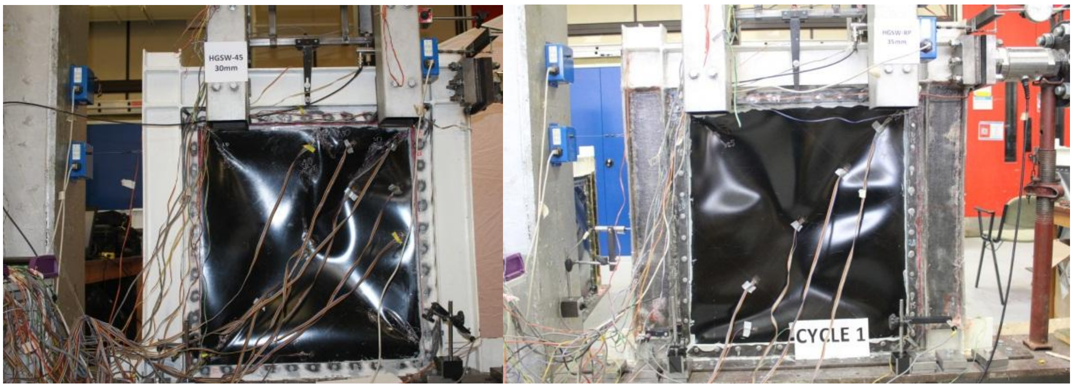

(a) **(b)**

Figure 11. a) Pristine HSGSW-P specimen after loaded to 30 mm displacement b) retrofitted HSGSW-R specimens after loaded to 35 mm displacement.

In retrofitted HSGSW-R specimen (Figure 11b), diagonal tension field action became visible at 2.5 mm displacement, which did not fully recover at the end of the loading cycle. First sign of cracking in the adhesive layer between fish plates and infill plate was noticed at the displacement of 10 mm. Delamination of the GFRP layer from steel infill plate started at displacement loading of 15 mm at the top corners. Development of the plastic hinges at the bottom of the columns was noticed at 20 mm displacement, which led to the debonding of the GFRP fabric from the columns. Snapping of the infill plate in the top corners occurred at the same level of displacement of 30 mm as in the pristine HSGSW-P specimen. At 30 mm displacement, plastic hinges were developed at top of the column; it also led to the debonding of the CFRP laminates around the top sections of the columns. Additionally crack in the connection between beam and column appeared. As the crack further progressed, the test was terminated at the end of first cycle of 35 mm displacement. GFRP delamination area from steel infill plate was smaller in comparison with pristine HSGSW-P specimen.

4.2 Load - displacement results

The load-displacement behaviours of pristine and retrofitted specimens are compared in Figures 12, 13 and 14 to investigate the opportunity for effective structural repair of steel and hybrid shear wall systems after they were subjected to seismic loading. Loads were calculated by taking the average from the extreme values of the cycles at the same displacement amplitude. The presented diagrams in Figures 12, 13 and 14 is an envelope from those average values.

Up to 10 mm displacements, for SSW-P and SSW-R specimens (Figure 12) the load values for corresponding displacements are approximately the same. The highest difference of 22% was recorded at 25 mm displacement in load values in favour of retrofitted specimen. Maximum load for the whole range of displacements for SSW-P was 285 kN and for SSW2 was 336 kN.

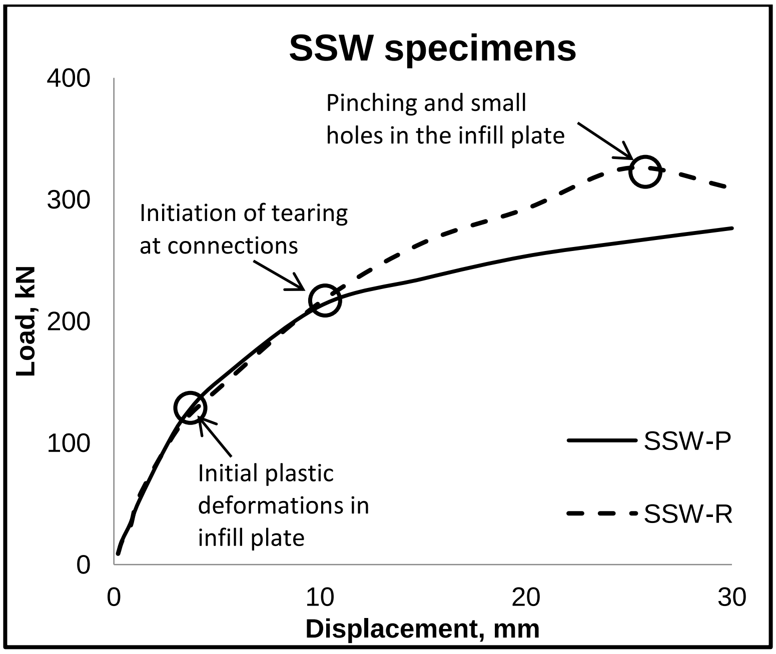

Figure 12. Load-displacement results for pristine SSW-P and retrofitted SSW-R specimens.

For HSCSW-P and HSCSW-R specimens (Figure 13), load values are nearly the same up to 7 mm displacement. In retrofitted HSCSW-R specimen larger increase in load was recorded for displacements between 7 mm and 15 mm displacements compared with HSCSW-P specimen. Above 15 mm displacement, load values was dropping for both specimens, however load values for retrofitted specimens were more than 10% higher compared to HSCSW-P specimen. HSCSW-R specimen achieved higher ultimate load in comparison with pristine HSCSW-P specimen, the difference in the ultimate load was recorded as 11% at 15 mm displacement.

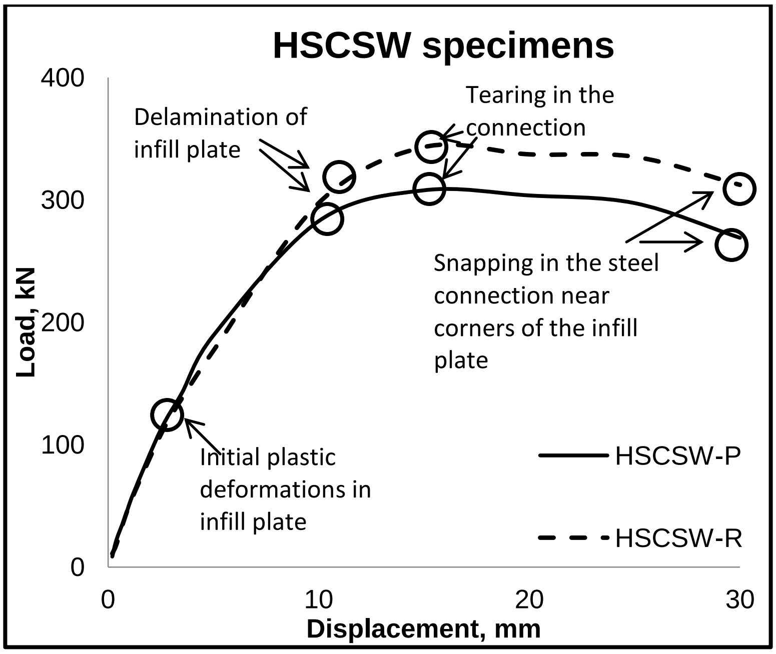

Figure 13. Load-displacement results for pristine HSCSW-P and retrofitted HSCSW-R specimens.

For HSGSW-P and HSGSW-R specimens (Figure 14) load value were approximately the same up to 5 mm displacement. At displacements between 5 mm and 15 mm, load values were higher for retrofitted HSGSW-R specimen in comparison with HSGSW-P. The highest load increase of 20% was recorded at 15 mm and at 30 mm displacements compared to pristine HSGSW-P specimen. The difference in ultimate load between retrofitted HSGSW-R and pristine HSGSW-P specimens was 14%.

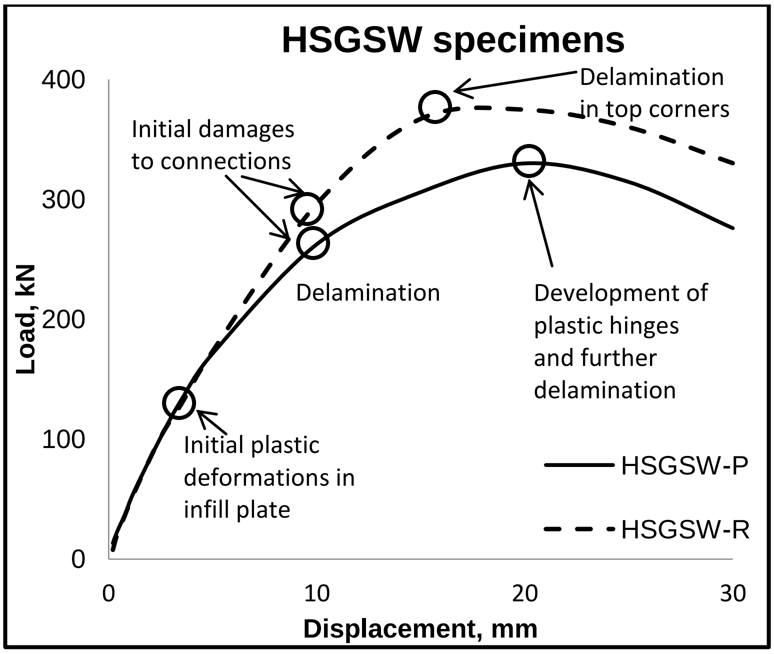

Figure 14. Load-displacement results for pristine HSGSW-P and retrofitted HSGSW-specimens.

For all types of the specimens, structural repair discussed above gave better results in respect of load values, ultimate load values and energy dissipation than the pristine specimens in the interval between 10 mm and 30 mm displacements.

Figure 15 compares load carrying capacity of pristine and retrofitted specimens starting at 5 mm displacement loading. From the behaviour of these two groups of specimens, it is noted that pristine and retrofitted hybrid carbon and hybrid glass have higher loading capacity than SSW specimens at every level of displacement loading. At 30 mm applied displacement due to significant delamination of FRP from infill plates in the direction of the tension field action, the behaviour of HSWs and SSW are nearly the same. Petkune et al. stated [20] that the use of the hybrid infill plates improves ultimate load values significantly. The same pattern of higher load carrying capacity for HSW specimens compared to SSW specimen was noted for retrofitted specimens.

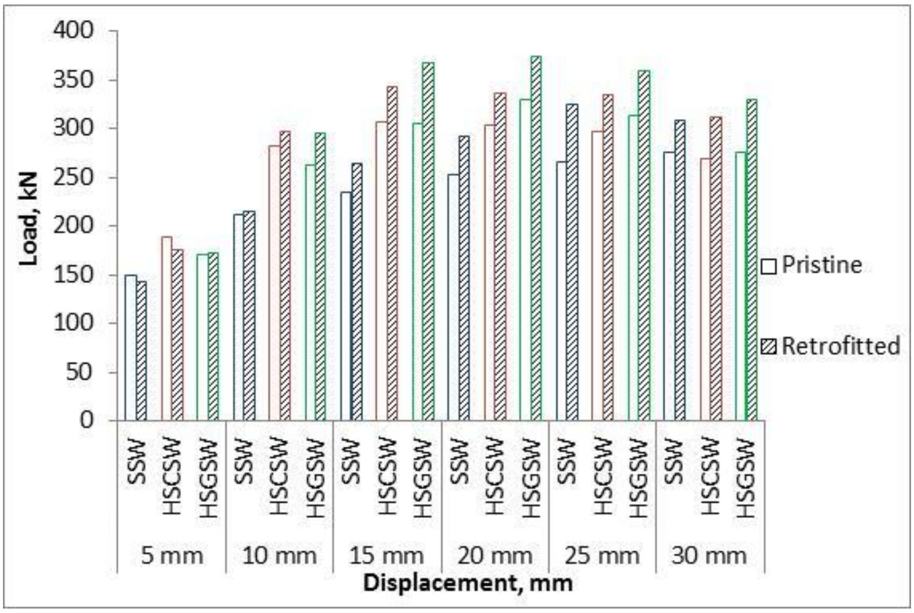

Figure 15. Comparison of the load-displacement results of different shear wall systems.

4.3 Energy dissipation in different types of shear wall specimens

Figure 16a shows energy dissipation for pristine and retrofitted specimens SSW, HSCSW and HSGSW at different stages of cyclic loading. The energy dissipation was calculated from measuring the area within all applied hysteresis loops. An example of the hysteresis loop for hybrid carbon and hybrid glass specimens at 25 mm displacement is shown in Figure 16b.

In the retrofitted SSW-R specimen energy dissipation relative to the pristine specimen is higher between 10 mm and 30 mm displacement, difference in values reaching 1.418 kJ at 30 mm displacement mainly due to increased thickness of the infill plate.

For hybrid specimens, energy dissipation in pristine and retrofitted ones were approximately the same; the biggest decrease of energy dissipation around 0.6 kJ for retrofitted specimen in comparison with pristine specimen was recorded at 15 mm displacements. Both retrofitted hybrid specimens had an increase in energy dissipation at 30 mm displacement, retrofitted HSCSW-R had 0.53 kJ increase and retrofitted HSGSW-R had an increase of 0.982 kJ relative to SSW specimen.

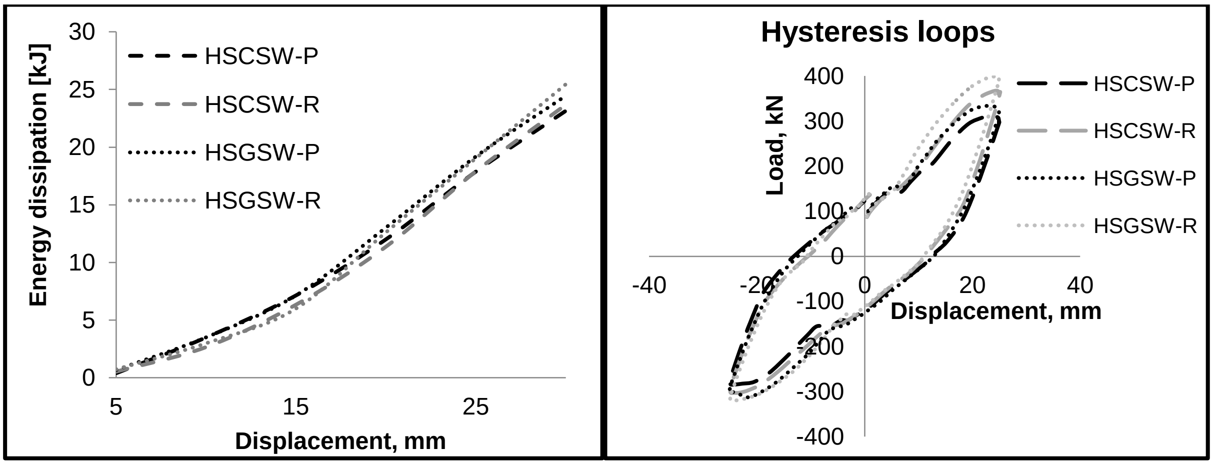

(a) (b)

Figure 16. Energy dissipation in hybrid specimens: a) energy dissipation between 5mm and 30 mm b) hysteresis loops for hybrid specimens at 1st cycle of 25 mm displacement loading.

The differences in energy dissipation values for all specimens at different stages of loading are summarised in Figure 17. Energy dissipation increases continuously from 5 mm to 30 mm displacement in all specimens. Previous studies [20] showed that energy dissipation in pristine hybrid specimens is higher than in steel specimens. The same tendency has been observed for retrofitted specimens between 15 mm and 30 mm displacements loading, and the highest result is achieved in retrofitted HSGSW-R specimen.

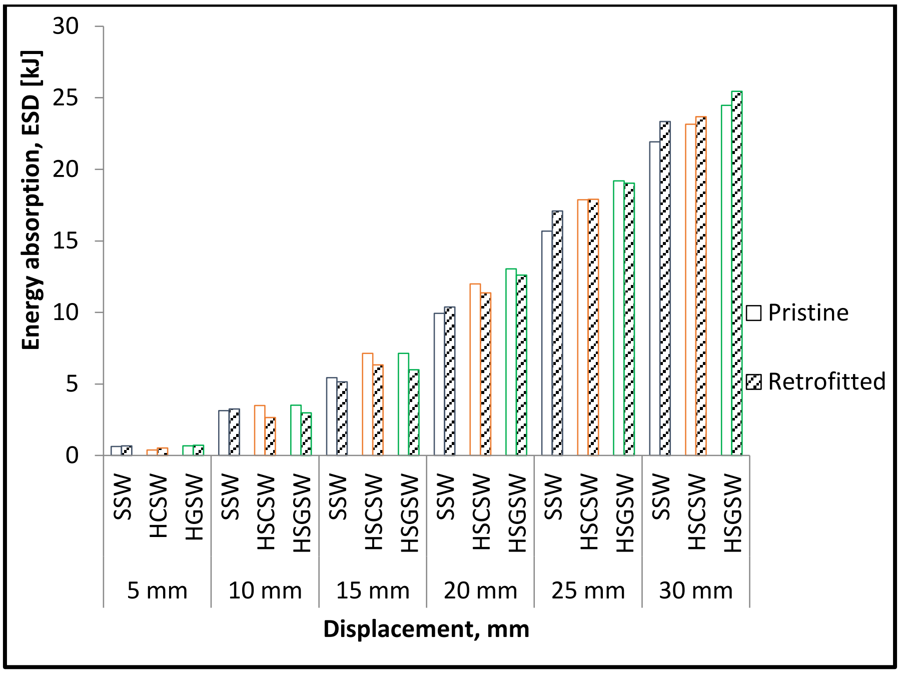

Figure 17. Comparison of energy dissipation in different types of shear wall specimens.

6 CONCLUSIONS

In this work scaled models of pristine steel and hybrid FRP shear walls were tested and after structural repair of the columns with CFRP laminates and GFRP fabric and replacement of the infill plates with new ones, retrofitted specimens were retested. From the test results the following conclusions can be made:

- Hybrid steel/CFRP and steel/GFRP shear walls have higher ultimate load in comparison with steel shear wall system within the applied levels of loading for both groups of tested specimens.
- Using the structural repair procedure outlined in the paper, resulted in higher ultimate load in retrofitted samples in comparison with pristine specimens.
- After retrofitting of the hybrid shear walls, the increases of load values are up to 16% higher for HSCSW and up to 20% higher for HSGSW. Corresponding increases of the ultimate load are 11% for HSCSW and 14% for HSGSW specimens.

- The energy dissipation of retrofitted specimens is very close to energy dissipation of the pristine specimens. The differences for cumulative energy dissipation between them during the full spectrum of loading are less than 10%.

In summary it has been shown that the proposed methodology for the retrofitting of damaged shear walls by bonding FRP materials to the frame and replacement of the infill plate is effective for all three configurations of specimens and the restored shear wall performance is as good as the pristine one.

Acknowledgement

The authors are grateful for the financial support from Kingston University London and would like to express gratitude to lab technicians in Structural, Composite and Materials Laboratories at Kingston University.

REFERENCES

[1] T. Roberts, “Seismic resistance of steel plate shear walls, Engineering Structures,” vol. 17, no. 5, pp. 344-351, 1995.

[2] J. W. Berman and M. Bruneau, “Experimental investigation of light-gauge steel plate shear walls,” *J. Struct. Eng.,* vol. 131, no. 2, p. 259–267, 2005.

[3] A. Rahai and M. Alipour, “Behavior and Characteristics of Innovative Composite Plate Shear Walls,” *Procedia Engineering,,* vol. 14, pp. 3205-3212, 2011.

[4] S. Rizkalla, M. Dawood and D. Schnerch, “Development of a carbon fiber reinforced polymer system for strengthening steel structures,” *Composites: Part A,* vol. 39, pp. 388-397, 2008.

[5] J. Teng, T. Yu and D. Fernando, “Strengthening of steel structures with fiber-reinforced polymer composites,” *Journal of Construction Steel Research,* vol. 78, pp. 131-143, 2012.

[6] X.-L. Zhao and L. Zhang, “State-of-the-art review on FRP strengthened steel structures,” *Engineering Structures,* vol. 29, pp. 1808-1823, 2007.

[7] A. Harries, A. Peck and E. Abraham, “Enhancing stability of structural steel sections using FRP,” *Thin-Walled Structures,* vol. 47, pp. 1092-1101, 2009.

[8] S. El-Tawil, E. Ekiz, S. Goel and S.-H. Chao, “Retraining local and global buckling behavior of steel plastic hinges using CFRP,” *Journal of Construction Steel Research,* vol. 67, p. 261–269, 2011.

[9] D. Schnerch and Rizkalla S., “Flexural strengthening of steel bridges with high modulus CFRP strips,” *Journal of Bridge Engineering,* vol. 13, no. 2, p. 192–201, 2008.

[10] E. Ghafoori, M. Motavalli, X.-L. Zhao, A. Nussbaumer and M. Fontana, “Fatigue design criteria for strengthening metallic beams with bonded CFRP plates,” *Engineering Structures,* vol. 101, pp. 542-557, 2015.

[11] Q. Yu, T. Chen, X. Gu, X. Zhao and Z. Xioa, “Fatigue behaviour of CFRP strengthened steel plates with different degrees of damage,” *Thin-Walled Structures,* vol. 69, pp. 10-17, 2013.

[12] M. Lesani, M. Bahaari and M. Shokrieh, “FRP wrapping for the rehabilitation of Circular Hollow Section (CHS) tubular steel connections,” *Thin-Walled Structures,* vol. 90, pp. 216-234, 2015.

[13] T. Yu, Y. Hu and J. Teng, “FRP-confined circular concrete-filled steel tubular columns under cyclic axial compression,” *Journal of Constructional Steel Research,* vol. 94, pp. 33-48, 2014.

[14] J. Berman, O. Celik and M. Bruneau, “Comparing hysteretic behaviour of the light-gauge steel

] plate shear walls and braced frames," *Engineering Structures,* vol. 27, pp. 475-485, 2005.

[15] C. Li, K. Tsai, J. Chang and C. Lin, "Cyclic Test of a Coupled Steel Plate Shear Wall Substructure. The Twelfth East Asia-Pacific Conference on Structural Engineering and Construction," *Procedia Engineering,* vol. 14, pp. 582-589, 2011.

[16] M. Alinia and M. Dastfan, "Behaviour of thin steel plate shear walls regarding frame members," *Journal of Constructional Steel Research,* vol. 62, pp. 730-738, 2006.

[17] A. Maleki, T. Donchev, H. Hadavinia and M. Limbachiya, "Improving the seismic resistance of structure using FRP/steel shear walls," in *Proceedings of 6th international Conference on Fiber Reinforced Polymer (FRP) Composites in Civil Engineering (CICE2012)*, Rome, Italy, 2012.

[18] F. Nateghi-Alahi and M. Khazaei-Poul, "Experimental study of steel plate shear walls with the infill plates strengthened by GFRP laminates," *Journal of Construction Steel Research,* vol. 78, pp. 159-172, 2012.

[19] F. Hatami, A. Ghamari and A. Rahai, "Investigating the properties of steel shear walls einforced with Carbon Fiber Polymers (CFRP)," *Journal of Construction Steel Research,* vol. 70, pp. 36-42, 2012.

[20] N. Petkune, T. Donchev, H. Hadavinia, M. Limbachiya and D. Wertheim, "Investigation of the behaviour of hybrid steel and FRP shear walls," in *Proceedings of 7th international Conference on Fiber Reinforced Polymer (FRP) Composites in Civil Engineering (CICE2014)*, Vancouver, Canada, 2014.

[21] N. Petkune, T. Donchev, H. Hadavinia and M. Limbachiya, "Investigation in connections between steel, composite and hybrid structural elements," in *Proceedings of MCM-2014: Mechanics of composite materials conference*, Riga, Latvia, June 2014.

[22] N. Petkune, T. Donchev, D. Wertheim, M. Limbachiya and H. Hadavinia, "Application of infrared thermography for assessment of condition of structural element," in *SMAR 2013: Second Conference on Smart Monitoring Assessment and Rehabilitation of Civil Structures*, Istanbul, Turkey., September 2013.

[23] N. Petkune, T. Donchev, D. Wertheim, H. Hadavinia and M. Limbachiya, "The use of the IRT to assess Steel and FRP hybrid elements," in *SMAR 2015: Third Conference on Smart Monitoring Assessment and Rehabilitation of Civil Structures*, Antalya, Turkey, September 2015.

[24] N. Petkune, T. Donchev, D. Petkova, H. Hadavinia, M. Limbachiya and Y. Hussein, "Opportunities for strengthening of damaged steel shear walls," in *Proceedings of Conference on Civil Engineering Infrastructure Cased on Polymer Composites (CECOM)*, Krakow, Poland, November

2012.

[25] Weber, “Weber.Tec Force Carbon Plate,” in *Retrieved from http://www.netweber.co.uk/uploads/tx_weberproductpage/10.010_weber.tec_force_carbon_plate.pdf*, July 2008, Available online.

[26] Weber, “Weber.Tec force glass sheet,” in *Retrieved from http://www.netweber.co.uk/uploads/tx_weberproductpage/10.030_weber.tec_force_glass_sheet.pdf*, July 2008, Available online.

[27] ATC-24, “Guidelines for Seismic testing of components of steel structures,” Report 24, Applied Technology Council, Redwood City, CA, 1992.